

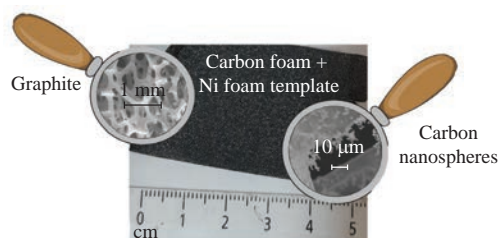
Energy characteristics of carbon spheres

Evgeniya V. Suslova,* Nikolay I. Osipov, Evgeniya V. Mashigina, Alina S. Viktorova,
Stepan Yu. Kupreenko, Oksana Ya. Isaikina and Sergey V. Savirov

Department of Chemistry, M. V. Lomonosov Moscow State University, 119991 Moscow,
Russian Federation. Fax: +7 495 939 3321; e-mail: suslova@kge.msu.ru

DOI: 10.1016/j.mencom.2021.01.029

The mixtures of template carbon foams and carbon spheres were synthesized by pyrolysis of hexane over Ni foam, followed by graphitization. All samples were analyzed by scanning and transmission electron microscopy, the BET method, thermogravimetry, Raman spectroscopy and X-ray diffraction. The standard enthalpy of formation of the presented material ($\Delta_f H_{298}^0 = 1.29 \pm 0.35 \text{ kJ g}^{-1}$) was determined for the first time.



Keywords: graphite, carbon foam, carbon spheres, graphitization, enthalpy of formation, bomb calorimetry.

Carbon foams (CFs) are the modern carbon materials with a three-dimensional graphitic structure, characterized by low density, high thermal conductivity and stability. These materials can be used for the manufacture of battery electrodes,¹ adsorbents of gases and metal ions, devices for saving thermal energy,² etc. One of the most common methods for the synthesis of CFs is a pyrolytic decomposition of hydrocarbons in the presence³ or absence⁴ of a template. Increasing the useful properties can be achieved by improving the crystalline structure of the material.⁵ The heat of combustion and the enthalpy of formation are fundamental characteristics of carbon nanomaterials (CNMs).^{6,7} In this work, we determined the standard enthalpy of formation ($\Delta_f H_{298}^0$) and compared it with that for graphite and various CNMs.

CFs were synthesized by chemical vapor deposition (CVD) *via* pyrolytic decomposition of hexane over Ni foam template[†] according to the described procedure.^{1,3} The physicochemical characteristics were investigated by scanning electron microscopy (SEM), transmission electron microscopy (TEM), the BET method, thermogravimetric (TG) and differential thermogravimetric (DTG) analyses, Raman spectroscopy and X-ray diffraction.[‡] CF morphology follows the shape of the Ni template [Figure 1(a)–(f)].

[†] The Ni foam was heated up to 900 °C in a horizontal quartz tube reactor with a diameter of 50 mm in an atmosphere of N₂–H₂ mixture (500:100 ml min⁻¹) for 5 min to remove the surface oxide layer. Then the N₂ stream (1000 ml min⁻¹) was bubbled through a flask with hexane before CVD at 900 °C for 1, 5, 15 or 30 min to give products designated as CF_1_0, CF_5_0, CF_15_0 and CF_30_0, respectively. After that, the supply of hexane was stopped and the products were graphitized in an atmosphere of N₂ at 900 °C for 15 or 30 min to afford products CF_5_15 and CF_5_30, respectively. The Ni template was removed by treating the products with HCl solution at room temperature for 8–10 h. The Ni template served as a catalyst and promoted the formation of the first few layers of graphite. The observed formation of new layers was much slower with increasing carbon thickness on the Ni surface.

[‡] SEM and TEM images were recorded on a JEOL JSM-6390LA scanning electron microscope and a JEOL 2100F/Cs transmission electron microscope, respectively. The specific surface area (S_{BET}) was measured by nitrogen adsorption using a Quantachrome AUTOSORB-1C/MS/TPR gas sorption analyzer. TG and DTG analyses were performed on an STA 409 PC

Increasing the synthesis or graphitization time to 15–30 min (samples CF_15_0, CF_30_0 and CF_5_30) resulted in the appearance of a noticeable amount of spherical carbon particles with a diameter of 1–1.6 μm on the CF surface [Figure 1(g),(h)]. Similar spherical particles were previously synthesized by CVD using C₂H₂ and a Ni catalyst⁸ or CH₄–H₂ and a Fe catalyst.⁹ According to the TEM image, the microstructure of materials

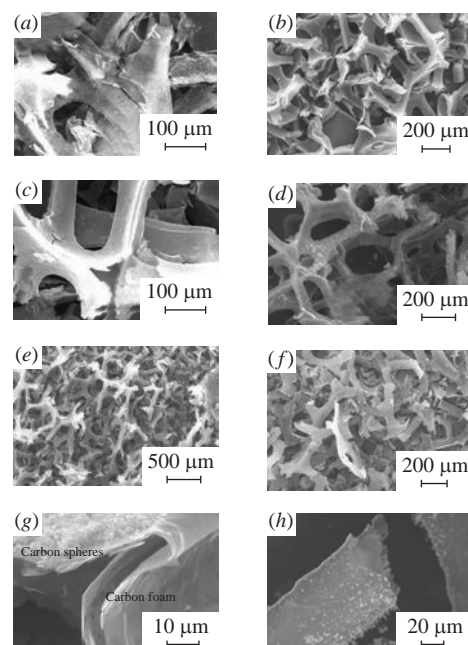


Figure 1 SEM images of (a) CF_1_0, (b) CF_5_0, (c) CF_15_0, (d) CF_30_0, (e) CF_5_15 and (f) CF_5_30 samples as well as carbon spheres on the surface of (g) CF_30_0 and (h) CF_5_30 samples.

LUXX thermal analyser at a heating rate of 5 °C min⁻¹ in air. X-ray diffraction patterns were recorded in the 2θ range from 20 to 60° on a Stadi-P instrument using CuKα₁ radiation. Raman spectra were recorded on a LabRam HR800 UV spectrometer with a 5 mW argon laser (514.5 nm).

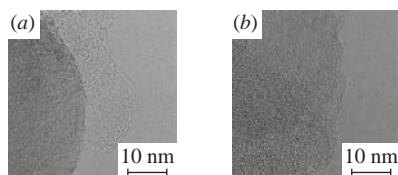


Figure 2 TEM images of (a) graphite domains and (b) amorphous phase in the CF_{5_0} sample.

consists of domains of structured graphite-like carbon [Figure 2(a)] and those of disordered carbon [Figure 2(b)].

The Ni template determined the morphology and the BET surface area of the obtained CFs. Adsorption isotherms indicated that S_{BET} values of both the Ni template and the CF_{5_0} sample were $16.2 \text{ m}^2 \text{ g}^{-1}$. The least thermally stable samples were CF_{15_0} and CF_{30_0}, which burned at 600–670 °C according to TG data [Figure 3(a)]. Graphitized samples CF_{5_15} and CF_{5_30} turned out to be the most resistant to oxidation since their ignition temperatures were 760–770 °C according to DTG data [Figure 3(b)]. Heat treatment improved the graphite structure, and the samples became more heat resistant. Samples CF_{1_0}, CF_{5_0}, CF_{15_0} and CF_{30_0} showed two extremes on the DTG curves [see Figure 3(b)]. This could be due to the heterogeneity of the sizes of the resulting graphite-like structures or the presence of a second phase, *i.e.*, carbon spheres. The ignition temperature of carbon nanospheres was previously defined as ~600 °C.⁹ The ignition temperature of bulk graphite was much higher and reached ~800 °C.

Figure 4 demonstrates XRD patterns. All CF samples had two characteristic carbon peaks at $2\theta = \sim 26^\circ$ (002) and $\sim 44^\circ$ (101). The peak of CF_{1_0} at $2\theta = 26.38^\circ$ ($d_{002} = 3.38 \text{ \AA}$) shifted with increasing synthesis time up to 5 min towards larger angles and reached $2\theta = 26.475^\circ$ ($d_{002} = 3.37 \text{ \AA}$). The d_{002} values were very close to those for graphite ($d_{002} = 3.34 \text{ \AA}$) and the previously described CFs^{4,10} or graphitized CFs^{11,12} (Table S1, see Online

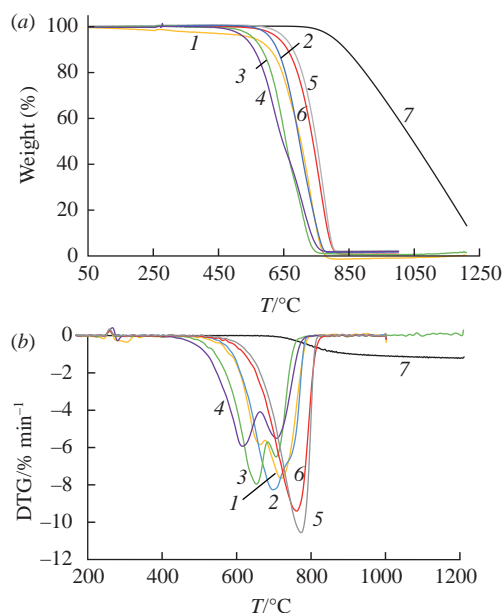


Figure 3 (a) TG and (b) DTG curves of (1) CF_{1_0}, (2) CF_{5_0}, (3) CF_{15_0}, (4) CF_{30_0}, (5) CF_{5_15} and (6) CF_{5_30} samples as well as (7) graphite.

[§] The heat of combustion $\Delta_c U$ was determined using an e2k isothermal bomb calorimeter. Pellets of CF (~0.2 g) were pressed with benzoic acid as an internal standard with the specific energy of combustion of $26.456 \pm 0.006 \text{ kJ g}^{-1}$ and placed onto a bomb of the calorimeter followed by filling 30 bar of O₂. The experiment was repeated six times to determine the statistical error.

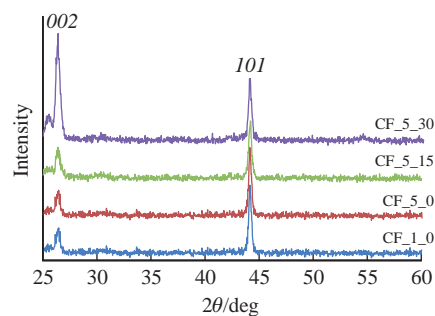


Figure 4 XRD patterns of CFs.

Supplementary Materials). Along with this, the d_{002} values increased for samples CF_{5_15} and CF_{5_30} (3.62 and 3.49 Å, respectively). Probably, the degree of disordering in these samples increased due to the appearance of carbon spheres in their composition.

The Raman spectra of carbon materials have three main lines: the D1 line at $\sim 1350 \text{ cm}^{-1}$ and the G line at $\sim 1580 \text{ cm}^{-1}$, corresponding to the A_{1g} and E_{2g} modes of the graphite lattice, and the D2 line at $\sim 2700 \text{ cm}^{-1}$, corresponding to the D1 overtone. The Raman spectra of the analyzed samples are shown in Figure 5. They were close to the spectra of graphite (samples CF_{1_0}, CF_{5_0} and CF_{15_0})¹³ and carbon spheres (samples CF_{30_0}, CF_{5_15} and CF_{5_30}).⁸ Graphite synthesized in 1 min was disordered and had only a few layers. Edge carbon atoms, which can be considered as defects, led to the appearance of the D1 line in the Raman spectra. The D1 line disappeared with an increase in the duration of the synthesis to 5 and 15 min. The appearance of wide D1 and G lines and the disappearance of the D2 line (samples CF_{30_0}, CF_{5_15} and CF_{5_30}) potentially indicated the presence of significantly disordered graphite-like planes,¹⁴ such as curved graphite planes expected in the structure of carbon spheres.⁸

Bomb calorimetry is a powerful method for the determination of $\Delta_f H_{298}^0$. Enthalpies of formation were determined for numerous CNMs. As a rule, $\Delta_f H_{298}^0$ strongly depends on CNM composition, size, structure, defectiveness, morphology and the presence of functional groups.^{6,15,16} The value of $\Delta_f H_{298}^0$ of carbon nanoparticles increases with decreasing size and with enhancing stress of their molecular structure. For example, $\Delta_f H_{298}^0$ is 8.60–21.70 kJ mol⁻¹ for carbon nanotubes,¹⁶ while for molecular fullerene C₆₀ $\Delta_f H_{298}^0 = 2288.5 \pm 16.2 \text{ kJ mol}^{-1}$.¹⁷

The experimental heat of combustion of CF_{5_0} was determined using an isothermal bomb calorimeter.⁸ The heat of combustion $\Delta_c U$ of the material was calculated after deducting the weight of water and impurities determined by TG [Figure 3(a) and Table 1]. Then, the enthalpies corresponding to metal oxidation were subtracted to obtain the enthalpy of combustion $\Delta_c H$ of the carbonaceous material using the following thermodynamic data:¹⁸

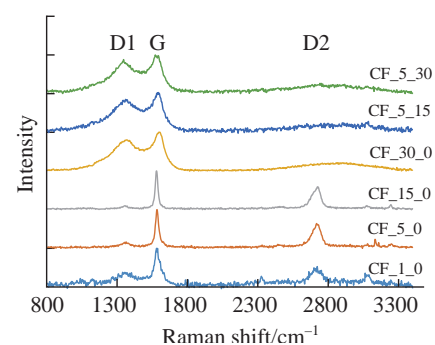
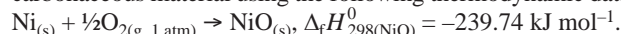


Figure 5 Normalized Raman spectra of CFs.

Table 1 The content of H₂O and Ni determined by TG, experimental heat of combustion ($\Delta_c U$), standard enthalpy of combustion ($\Delta_c H_{298}^0$) and specific standard enthalpy of formation ($\Delta_f H_{298}^0$) of CF_5_0.

Sample	H ₂ O (wt%)	Ni (wt%)	$\Delta_c U /$ kJ g ⁻¹	$\Delta_c H_{298}^0 /$ kJ g ⁻¹	$\Delta_f H_{298}^0 /$ kJ g ⁻¹
CF_5_0	0.01	1.81	33.52 ± 0.34	-34.08 ± 0.34	1.29 ± 0.35

The standard enthalpy of combustion $\Delta_c H_{298}^0$ was determined after the Washburn correction.^{6,15,16} The standard enthalpy of formation $\Delta_f H_{298}^0$ was calculated according to Hess's law: $\Delta_f H_{298}^0(\text{CF}_5_0) = \Delta_f H_{298}^0(\text{CO}_2) - \Delta_c H_{298}^0(\text{CNMs})$ using the following thermodynamic data:¹⁸ $\text{C}_{(\text{graphite})} + \text{O}_{2(\text{g}, 1 \text{ atm})} \rightarrow \text{CO}_{2(\text{g}, 1 \text{ atm})}$, $\Delta_f H_{298}^0(\text{CO}_2) = -32.79 \pm 0.01 \text{ kJ g}^{-1}$.

The $\Delta_f H_{298}^0$ value of the carbon materials investigated in this work was positive and equal to $1.29 \pm 0.35 \text{ kJ g}^{-1}$ (see Table 1). Taking into account that the enthalpy of formation of graphite is 0 kJ g^{-1} , positive values of the energy $\Delta_f H_{298}^0$ can be attributed to the carbon spheres contained in the materials under study.

The determination of $\Delta_f H_{298}^0$ is a suitable method for searching and proving approaches to the stabilization of CNMs. This work expands the understanding of the thermodynamic stability of CNM that is important for various applications of derived materials.

This work was supported by the Russian Foundation for Basic Research (project no. 19-03-00713a) and M. V. Lomonosov Moscow State University Program of Development. The authors thank S. V. Maximov for TEM images.

Online Supplementary Materials

Supplementary data associated with this article can be found in the online version at doi: 10.1016/j.mencom.2021.01.029.

References

- 1 E. Suslova, A. Viktorova, N. Osipov, K. Maslakov and N. Kuznetzova, *Funct. Mater. Lett.*, 2020, **13**, 2040003.
- 2 M. Inagaki, J. Qiu and Q. Guo, *Carbon*, 2015, **87**, 128.
- 3 Y. Xue, D. Yu, L. Dai, R. Wang, D. Li, A. Roy, F. Lu, H. Chen, Y. Liu and J. Qu, *Phys. Chem. Chem. Phys.*, 2013, **15**, 12220.
- 4 E. A. Rayskaya, O. B. Belskaya and V. A. Likholobov, *Mater. Today: Proc.*, 2018, **5**, 25962.
- 5 J. Marx, H. Beisch, S. Garlof and B. Fiedler, *Advanced Material Science*, 2017, **2** (4), 1.
- 6 E. V. Suslova, S. V. Savilov, J. Ni, V. V. Lunin and S. M. Aldoshin, *Phys. Chem. Chem. Phys.*, 2017, **19**, 2269.
- 7 S. Savilov, N. Cherkasov, M. Kirikova, A. Ivanov and V. Lunin, *Funct. Mater. Lett.*, 2010, **3**, 289.
- 8 C. N. Hunter, M. H. Check, C. H. Hager and A. A. Voevodin, *Tribol. Lett.*, 2008, **30**, 169.
- 9 P. Serp, R. Feurer, P. Kalck, Y. Kihn, J. L. Faria and J. L. Figueiredo, *Carbon*, 2001, **39**, 621.
- 10 A. N. Popova, *Coke Chem.*, 2017, **60**, 361 (*Koks Khim.*, 2017, no. 9, 32).
- 11 R. Mehta, D. P. Anderson and J. W. Hager, *Carbon*, 2003, **41**, 2174.
- 12 J. Rodríguez-García, I. Cameán, A. Ramos, E. Rodríguez and A. B. García, *Electrochim. Acta*, 2018, **270**, 236.
- 13 A. C. Ferrari, *Solid State Commun.*, 2007, **143**, 47.
- 14 A. Kaniyoor and S. Ramaprabhu, *AIP Adv.*, 2012, **2**, 032183.
- 15 E. V. Suslova, K. I. Maslakov, S. V. Savilov, A. S. Ivanov, L. Lu and V. V. Lunin, *Carbon*, 2016, **102**, 506.
- 16 N. B. Cherkasov, S. V. Savilov, A. S. Ivanov and V. V. Lunin, *Carbon*, 2013, **63**, 324.
- 17 A. Rojas-Aguilar, *J. Chem. Thermodyn.*, 2002, **34**, 1729.
- 18 M. W. Chase, *NIST-JANAF Thermochemical Tables*, 4th edn., American Institute of Physics, New York, 1998.

Received: 9th September 2020; Com. 20/6307